KERNFORSCHUNGSZENTRUM

KARLSRUHE

August 1970

KFK 1055

Institut für Experimentelle Kernphysik

Investigation of T=0 Excited States of ^{4}He Using Three-Particle Reactions

E. L. Haase, R. Hagelberg, W. N. Wang, E. K. Lin,
D. P. Saylor, M. A. Fawzi

GESELLSCHAFT FÜR KERNFORSCHUNG M. B. H.

KARLSRUHE

KERNFORSCHUNGSZENTRUM KARLSRUHE

August 1970 KFK 1055

Institut für Experimentelle Kernphysik

Investigation of T=0 Excited States of ^{4}He Using Three-Particle Reactions

E.L. Haase, R. Hagelberg, W.N. Wang[+], E.K. Lin[+], D.P. Saylor and M.A. Fawzi

Gesellschaft für Kernforschung m.b.H. Karlsruhe

Papers G-26 and K-83 presented at the Joint Spring Meeting of the Nuclear Physics Section of the German and Dutch Physical Societies in Eindhoven, Netherlands, April 1970

[+] On leave from the Institute of Physics, Academia Sinica, and Tsing Hua University, Taiwan, China.

Abstract

Using 52 MeV deuterons and 104 MeV α-particles coincidence measurements in three entrance channels were carried out for the following reactions:

$^{4}He(d,d't)^{1}H$	$^{4}He(\alpha,\alpha't)^{1}H$	$^{6}Li(d,\alpha't)^{1}H$
	$^{4}He(\alpha,\alpha'^{3}He)n$	$^{6}Li(d,\alpha'^{3}He)n$
$^{4}He(d,d'd)D$	$^{4}He(\alpha,\alpha'd)D$	$^{6}Li(d,\alpha'd)D$

In measuring the correlations, the detector of the inelastic particle was kept at a fixed position and the second detector scanned over a range of coplanar angles favouring ^{4}He final state interactions.

The data can be fitted consistently with six T=0 excited states of ^{4}He, at 20.2 MeV, 21.1 MeV, 21.9 MeV, 25.5 MeV, 28.5 MeV and 31.8 MeV with widths (Γ) of 0.2 MeV, 0.8 MeV, 1.8 MeV, 2.9 MeV, 5.3 MeV and 5.6 MeV respectively. The validity of the sequential reaction mechanism is examined. The internal consistency of the level parameters for the three entrance and three decay channels as well as the symmetry of the extracted angular correlations about 0 and 90^{o} in the recoil system centre of mass agree very well with the model of sequential decay. The angular correlations agree well with the predictions of a simple theory using the impulse approximation.

Zusammenfassung

Dreiteilchenreaktionen mit 52 MeV Deuteronen und 104 MeV α-Teilchen wurden mit drei Eingangskanälen für die folgenden Reaktionen untersucht:

$^4He(d,d't)^1H$	$^4He(\alpha,\alpha't)^1H$	$^6Li(d,\alpha't)^1H$
	$^4He(\alpha,\alpha'^3He)n$	$^6Li(d,\alpha'^3He)n$
$^4He(d,d'd)D$	$^4He(\alpha,\alpha'd)D$	$^6Li(d,\alpha'd)D$

Die Winkelkorrelation wurde koplanar gemessen mit einem festgelegten Detektor für die inelastischen Teilchen und einem zweiten Detektor, der einen Winkelbereich überfuhr, in dem die ^4He Endzustandswechselwirkung bevorzugt auftritt.

Die Meßdaten werden für alle Reaktionen gut angepaßt durch sechs T = 0 Zustände des ^4He - Kerns, bei 20,2 MeV, 21,1 MeV, 21,9 MeV, 25,5 MeV, 28,5 MeV und 31,8 MeV mit Breiten (Γ) von 0,2 MeV, 0,8 MeV, 1,8 MeV, 2,9 MeV, 5,3 MeV und 5,6 MeV.

Die Gültigkeit des sequentiellen Reaktionsmechanismus wird erörtert. Sowohl die fast gleichen Werte der Resonanzparameter für die drei Eingangs- und die drei Zerfallskanäle als auch die Tatsache, daß die Winkelkorrelation im Schwerpunkt des Rückstoßsystems symmetrisch um 0° und um 90° ist, stimmen gut mit dem Modell des sequentiellen Zerfalls überein. Eine einfache Theorie, welche auf der Impuls-Approximation basiert, gibt die Winkelkorrelation gut wieder.

Contents

1. Introduction

The ^{4}He nucleus is the lightest nucleus with an extensive system of excited states. It is a doubly magic nucleus with a high degree of symmetry. These facts have stimulated a number of theoretical calculations in recent years [1 - 7]. The splittings of the 7 members of the ℓ=1 supermultiplet yield information on the strength of tensor forces [3]. Also model independent calculations starting from nucleon-nucleon forces are now coming within the realm of possibilities [7].

The fact that all the excited states in ^{4}He are particle unstable and that their widths are appreciable in comparison with their energies above threshold make both measurements and interpretation of ^{4}He resonances difficult. So far practically all of the information on resonances in the mass 4 system has been obtained from phase-shift analyses of elastic scattering and of reactions, proceeding through a mass 4 compound nucleus [8]) (fig. 1a).

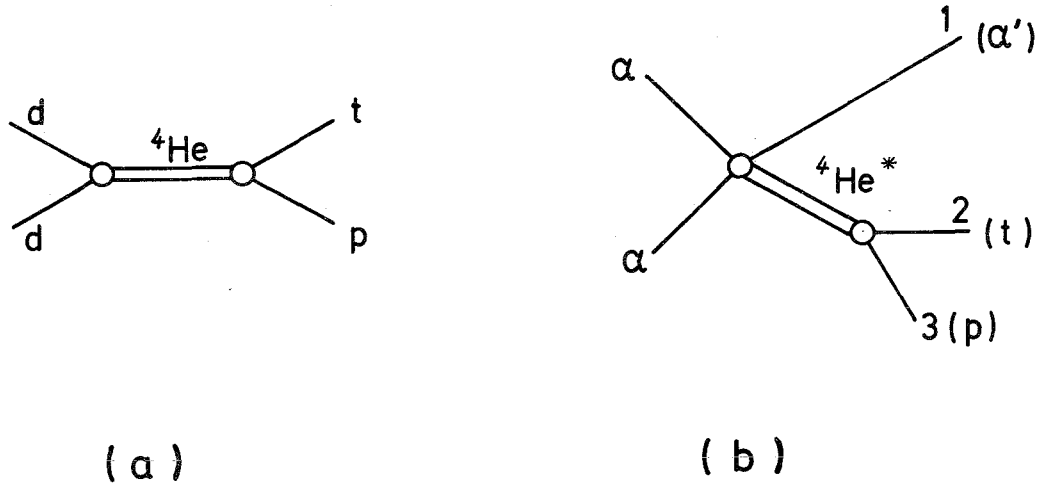

Fig. 1. Diagrams (a) for a reaction and (b) for a reaction with three particles in the exit channel, both forming ^{4}He* as intermediate system.

An alternate approach is to study reactions with three particles in the exit channel in which ^{4}He resonances appear through final state interactions (FSI) between a pair of the outgoing particles.

Here $^{4}He^{*}$ is formed in a direct reaction and decays into one of the three possible decay channels T+p(Q=19.81 MeV), ^{3}He+n(Q=20.58 MeV) and d+d(Q=23.84 MeV above the ^{4}He ground state). The assumption of sequential decay appears reasonable at our incident energies. During the mean life of the lowest excited state the inelastic particle and the intermediate system separate by about 100 times the range of their nuclear interaction. Conservation of isospin and parity, and possibly the reaction mechanism, lead to considerable selectivity in the levels that can be excited. This is a great help in untangling the overlapping resonances. The problem of overlap between the 21.1 MeV, 0^{-} and the 21.9 MeV, 2^{-} states is particularly severe. As the 0^{-} state is forbidden on account of parity conservation in the inelastic scattering of α-particles off ^{4}He, this reaction offers a unique possibility to determine level parameters for the 2^{-}, T=0 state. Previous [14,15]) kinematically complete experiments have only been able to positively identify the 20.2 MeV, 0^{+} state. Reactions with three particles in the exit channel lend themselves to a reasonably simple interpretation if the reaction proceeds via sequential decay. To test the validity of this hypothesis of sequential decay and to extend the available information on excited states of the α-particle is the aim of the present work. It attempts also to extract the energy and width of higher excited states of ^{4}He. To this end we investigated the following reactions using 104 MeV α-particles and 52 MeV deuterons:

$^{4}He(\alpha,\alpha't)^{1}H$	$^{6}Li(d,\alpha't)^{1}H$	$^{4}He(d,d't)p$
$^{4}He(\alpha,\alpha'^{3}He)n$	$^{6}Li(d,\alpha'^{3}He)n$	$^{4}He(d,d'd)D$
$^{4}He(\alpha,\alpha'd)D$	$^{6}Li(d,\alpha'd)D$	

Within the validity of isospin conservation all three entrance channels excite only T=0 levels.

Preliminary data contained in the present work have previously been published [9]).

2. Kinematics and Experimental Procedure

In discussing the kinematics we follow the notation of Ohlson [10]. Let us consider coplanar events, as all present measurements were done in the reaction plane. A projectile p is inelastically scattered off the target t and emerges as particle 1 at the laboratory angle θ_1^l (fig. 2). If for convenience we treat the reaction as sequential, the intermediate system 2-3 recoils in the direction θ_{23}^l and carries a definite energy E_{23} above the two-particle threshold. This corresponds to a definite excitation

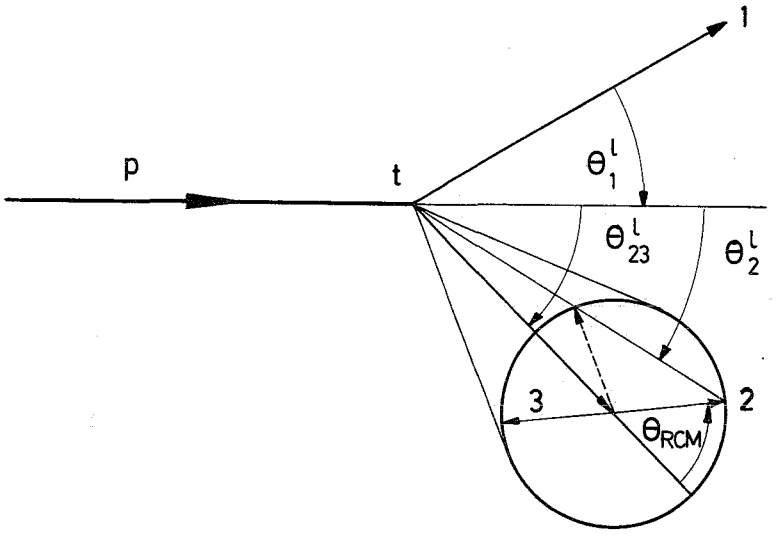

Fig. 2. Kinematics of sequential decay.
t=target, p=projectile.

energy $E_x=E_{23}+Q$ referred to its ground state. The intermediate system then decays into two particles forming an angle $\theta_{RCM}(=\theta^{c'(1)})$ with the recoil axis in its centre of mass system, and the energy E_{23} is shared by the particles 2 and 3. The recoil momentum combines with the momentum set free in the decay, so particle 2 emerges at θ_2^l. In the case $E_{23} < E_{Recoil}$, for a given E_{23} particle 2 (having mass 2 or mass 3) can only emerge within a definite decay cone.

To a given θ_2^l generally two values of θ_{RCM} are associated, one for θ_{RCM} less than about 90^o and another (shown dashed in fig. 2) for θ_{RCM} larger than about 90^o.

To gain "kinematically complete" information we have carried out coincidence measurements between the inelastic particle 1 and the decay particle 2, simultaneously measuring T, ^{3}He and d for the three possible 2-particles decay channels. θ_1^l was kept fixed and θ_2^l was varied in up to 20 steps over a range of angles favouring ^{4}He final state interactions. After transformation into the recoil system center of mass (RCM), one obtains the angular correlation in the RCM system. The beam of 104 MeV α-particles and 52 MeV deuterons was provided by the Karlsruhe Isochronous cyclotron.

Fig. 3. Map display of raw data. From left to right, events lie along the kinematic curves for the ^{4}He(α,α'd)D, ^{4}He(α,α't)^{1}H and ^{4}He(α,α'^{3}He)n reactions.

Fig. 3 shows a typical map display of a two-parameter coincidence measurement for the inelastic α-scattering off ^{4}He. One can see events along the kinematically allowed curves for the three decay modes. For the triton curve one can see in addition to the upper branch (large E_2^l, $\theta_{RCM} < \approx 90^o$) also the lower branch (small E_2^l, $\theta_{RCM} > \approx 90^o$). Using ^{4}He gas and ^{6}Li self-supporting targets, data were recorded for the eight reactions investigated.

To facilitate particle identification, solid state detectors were used for both telescopes. Timing signals from the two telescopes were send to a start-stop time to amplitude converter. A discriminator window corresponding to 30 nsec was set on the output. This corresponds to about twice the value needed to compensate for time of flight differences. E_1^ℓ singles spectra, gated with the ORTEC particle identifier discriminator output, were recorded throughout the measurements simultaneously. E_2^ℓ singles gated with discriminator outputs for d, t, and ^{3}He windows on the E_2 particle identifier signal, measured for each θ_2^ℓ, permitted the small remaining correction for random coincidences to be carried out. The shift of the ^{3}He curve was carried out by adding a standard pulse to the E_2^ℓ signal when ever the ^{3}He discriminator triggered. For the ^{6}Li + d reactions all ADC outputs were also recorded event by event on magnetic tape for later analysis. The events are summed up across each ridge and are projected onto the $E_{\alpha'}$-axis; there is a definite, slightly non-linear relationship between $E_{\alpha'}$ and E_x for the resonances in ^{4}He.

3. Results and analysis of the energy distributions

3.1 The ^{4}He(α,α't)^{1}H reaction

Fig. 4 shows for fixed θ_1^ℓ as a function of E_x with θ_2^ℓ as parameter a representative set of spectra from projections of the upper branch for the ^{4}He(α,α't)^{1}H reaction. The transformation from $E_{\alpha'}^\ell$ to E_x has been carried out by multiplying with $\Delta E_1^\ell/\Delta E_x$. Just above the threshold at 19.81 MeV one notices the well known 0^+, 20.2 MeV state. It appears only within the limits between θ_2^ℓ=44.5° and θ_2^ℓ=56.3° of its decay cone. Outside the cone a broad peak at E_x=21.9 MeV can be seen. As the 0^- state at 21.4 MeV [8]) is forbidden on account of parity conservation (identical spin 0 bosons incident), this reaction is particularly suited to determine resonance parameters for the third (2^-, T=0) state of ^{4}He. Beyond that there is a broad structure peaking at 28.5 MeV. For increasing θ_2^ℓ this gets obscured by a peak moving in from the left and arising from the p-^{4}He FSI in the ground state. It occurs at the kinematically predicted positions. For changing θ_2^ℓ this peak must shift.

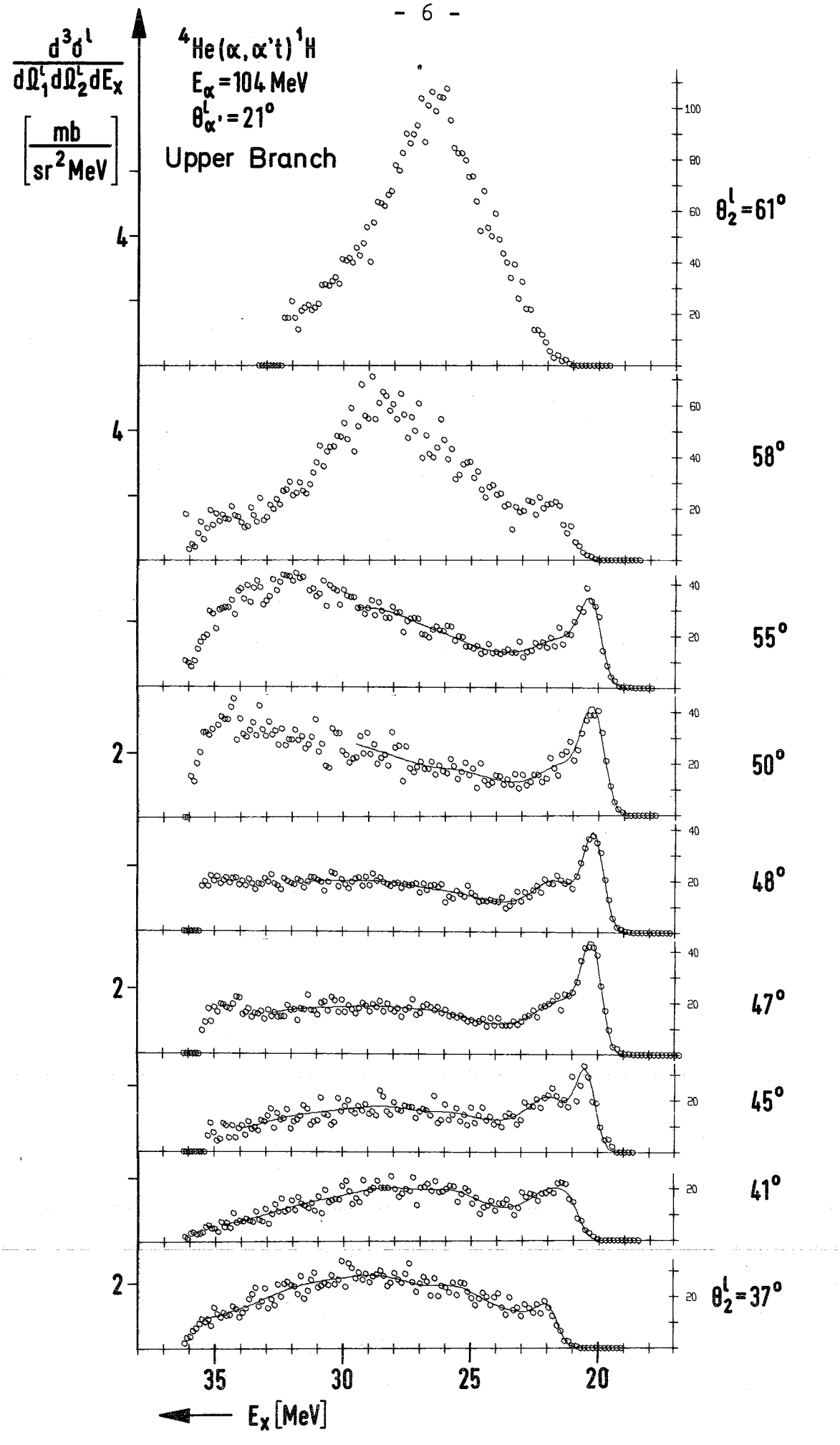

Fig. 4. Representative family of spectra for the $^4He(\alpha,\alpha't)^1H$ reaction as a function of excitation energy in ^4He.

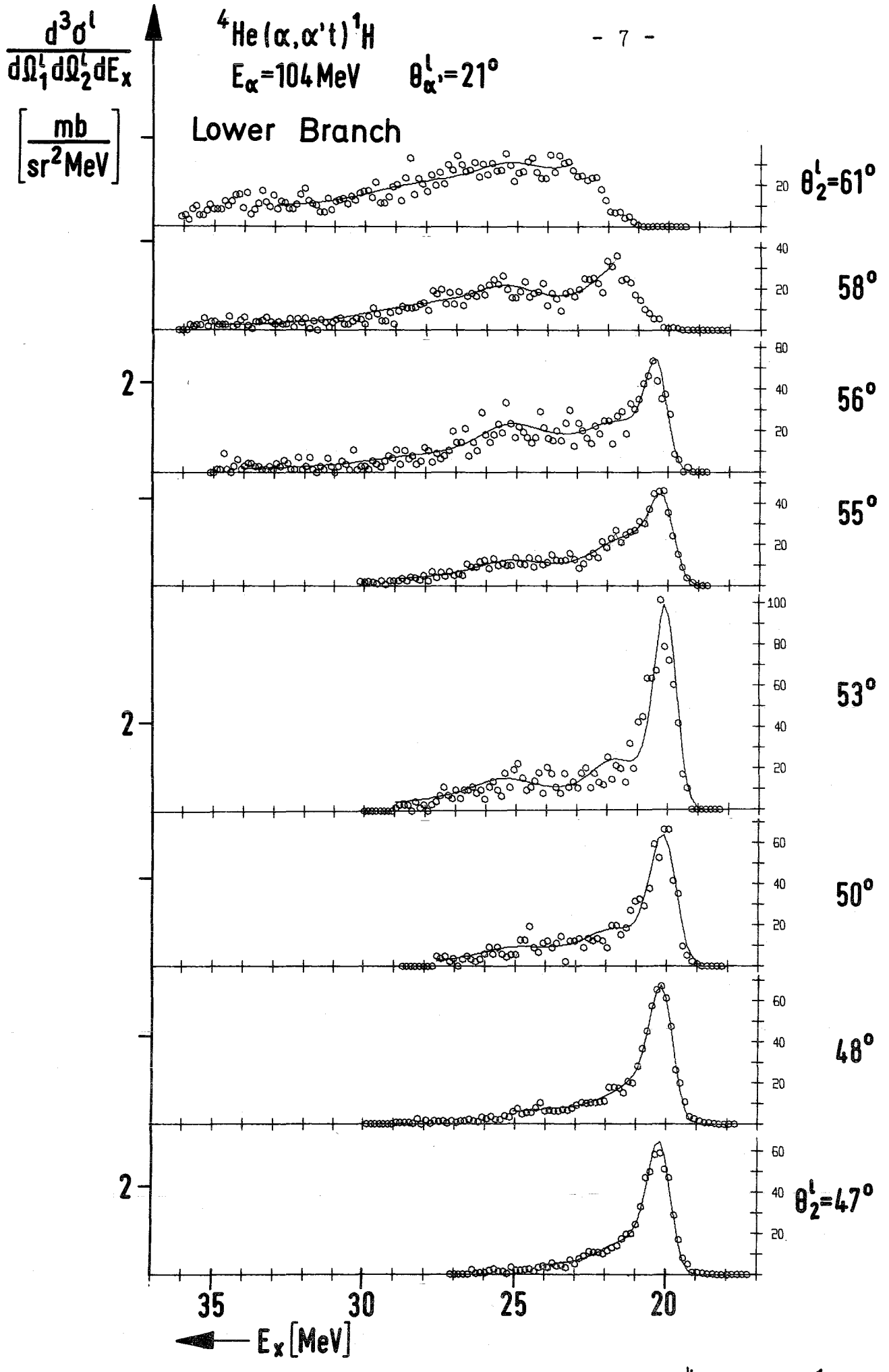

Fig. 5. Representative family of spectra for the $^4He(\alpha,\alpha't)^1H$ reaction as a function of excitation energy in ^4He.

Fig. 5 shows 8 spectra for the lower branch of the same reaction. The rapid fall of the phase-space distribution leads to a small laboratory cross section for higher excitation energies. Together with the increased random rate this makes evaluation for higher excitation energies more uncertain. Beyond the resonances at 20.2 and 21.9 MeV already noted for the upper triton branch, with increasing θ_2^ℓ another bump at 25.5 MeV starts coming up. The low energy regions of the two spectra for the largest values of θ_2^ℓ are partly disturbed by tails from ^{5}Li resonances.

3.2 Method of analysis and theoretical interpretation

Generally for each decay channel c we have

$$\frac{d^3\sigma_c^\ell}{d\Omega_1^\ell \, d\Omega_2^\ell \, dE_1^\ell} = |M_c|^2 \cdot \rho_c \simeq |U_c|^2 \cdot |M_c^{seq}|^2 \cdot \rho_c \qquad (1)$$

where ρ_c is the phase-space factor for the decay channel under consideration. The matrix element M_c combines both vertices in fig. 1b. Following Goldberger and Watson [11]) we factorise M_c into a term U_c independent of internal coordinates of the 2-3 system arising from the first vertex and an enhancement factor M_c^{seq} which describes the final state interaction between particles 2 and 3 and which reflects resonances in the 2-3 system. For the case of the PWBA this formula lends itself to a simple interpretation and permits explicit calculation of both energy and angular dependence:

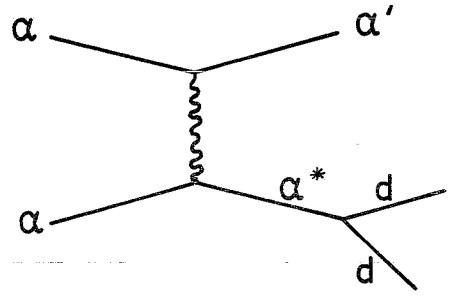

PWBA model of sequential reaction

Levinson [12]) and others have shown that the zero range PWBA treatment is formally identical with that of the exchange of a fictious spin-less particle. This has momentum along the recoil axis, and angular momentum ℓ relative to the target. Then we have the problem of the scattering of this fictious S=0 particle off an S=0 α-particle forming an intermediate state possessing a series of resonances with J^π decaying into the three possible decay channels.

This can be explicitly calculated in terms of the R-matrix theory or the theory of Humblet and Rosenfeld [13]. According to ref. [12] the use of DWBA and non-zero range forces does not materially alter the picture, but may lead to different populations of the magnetic substates of the intermediate system.

As a first step in analysing our data we neglect Coulomb and threshold effects, interferences between levels and coupling between decay channels. Then assuming the non-resonant coefficients with a smoothly varying energy dependence to be constants, the expression for the reaction-matrix element [13] reduces to

$$|M_c^{seq}(E_x,\Theta_{RCM})|^2 = \sum_{\ell=o}^{\ell_{max}} \left[C + \sum_n \frac{\frac{1}{2}\Gamma_n B_{\ell n} + (E_x - E_n) A_{\ell n}}{(E_x - E_n)^2 + \Gamma_n^2/4} \right] P_\ell(\cos \Theta_{RCM}) \qquad (2)$$

The sum over ℓ is limited to $\ell_{max} < 2J$ or $2L$, whichever is smaller; the $B_{\ell n}$ are zero for odd values of ℓ. The sum over n extends over all resonances of definite J^π. C is a constant non-resonant term, the B coefficients give the intensity of Breit-Wigner single level resonances, and the A coefficients give the intensity of interference between the resonances and the non-resonant background (limited in size so that the cross-section does not become negative).
Actually the data are measured in the laboratory system, and it is the simplest to carry out the fitting in that system also, because of the folding effect of the energy resolution. We have fitted the spectra for a set of values of Θ_2^ℓ for each of the reactions with the expression

$$\frac{d^3\sigma^\ell_{exp}}{d\Omega_1^\ell \, d\Omega_2^\ell \, dE_1^\ell} = F\left\{ \left[C(\Theta_2^\ell) + \sum_n \frac{\Gamma_n B_n(\Theta_2^\ell) + (E_x - E_n) A_n(\Theta_2^\ell)}{(E_x - E_n)^2 + \frac{1}{4}\Gamma_n^2} \right] \rho^\ell(E_1^\ell) \right\} . \qquad (3)$$

Here F denotes the operation of folding the "theoretical" curve with the experimental resolution, taken to have a gaussian form. The coefficients for each resonance n have been rewritten:

$$B_n(\theta_2^\ell) = \sum_\ell \frac{1}{2} B_{\ell n} P_\ell (\cos \Theta_{RCM}) \qquad (4)$$

$$A_n(\theta_2) = \sum_\ell \frac{1}{2} A_{\ell n} P_\ell (\cos \Theta_{RCM})$$

For the explicit form of $\rho^\ell(E_1^\ell)$ see formula (28) in ref [10]).
An automatic fitting program utilising an IBM 360-65 was developed. In fitting each family, resonance position as well as width parameters are varied in common and the B_n, A_n and C individually for each spectrum so as to minimize χ^2. The resulting fits are drawn as solid curves in the spectra.

As shown in fig. 4-6 and 9,10 excellent fits are obtained for all spectra. The value of $\chi_1^2 = \chi^2/(M-N)$ (χ^2 divided by the number of data points minus the number of parameters) ranges between 1.05 and 1.18 for the different families, as compared with expected value of 1.

In fitting the data, regions corresponding to excitation up to 5 MeV in ^{5}Li and ^{5}He were omitted, so as to exclude the mass 5 ground state and a possible weak first excited state around 2.6 MeV.

3.3 The ^{4}He(α,α'd)D reaction and transformation into the RCM system

Fig. 6 shows a representative set of spectra for the ^{4}He(α,α'd)D reaction. The small bump around 24 MeV excitation does not correspond to a resonance, but results from the shape of the projected phase-space distribution. (see fig. 7). As for the triton decay there is a broad maximum peaking around 28.5 MeV. This peak falls with increasing θ_2^ℓ and a structure is reached which certainly cannot be fitted with a single Breit-Wigner resonance.

For this reaction no quasielastic process is expected to contribute as the Q-value (~ 24 MeV) is rather large compared with the energy available in the centre of mass (52 MeV). Also its maximum at $\theta_2^\ell \approx 23^\circ$, $E_x \approx 43$ MeV would lie outside the region measured. There is no evidence for FSI arising from ^{6}Li resonances. They would show up as narrow, rapidly shifting peaks; though for the spectra for the largest values of θ_2^ℓ a small contribution cannot be excluded.

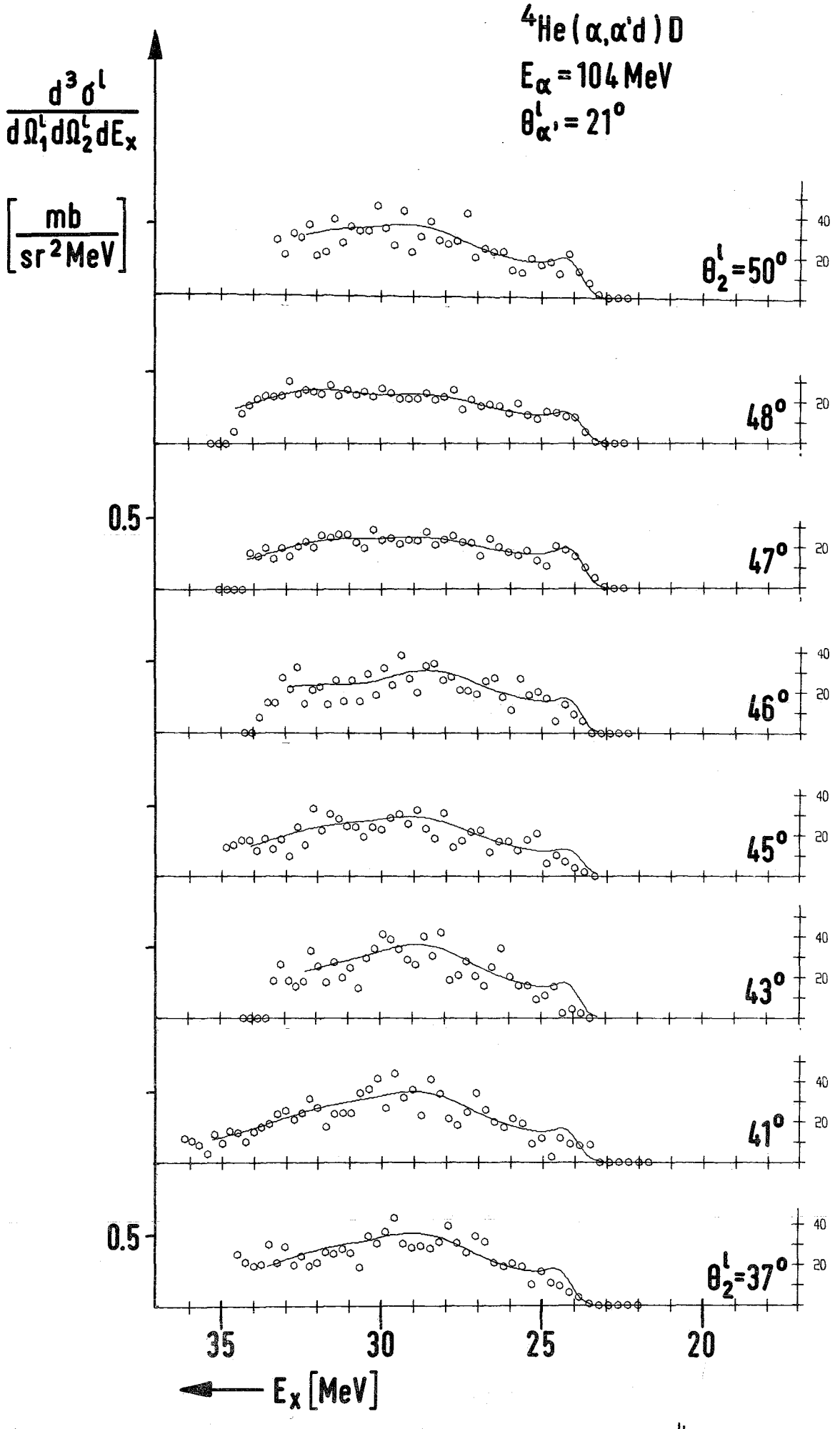

Fig. 6. Representative family of spectra for the $^4He(\alpha,\alpha'd)D$ reaction.

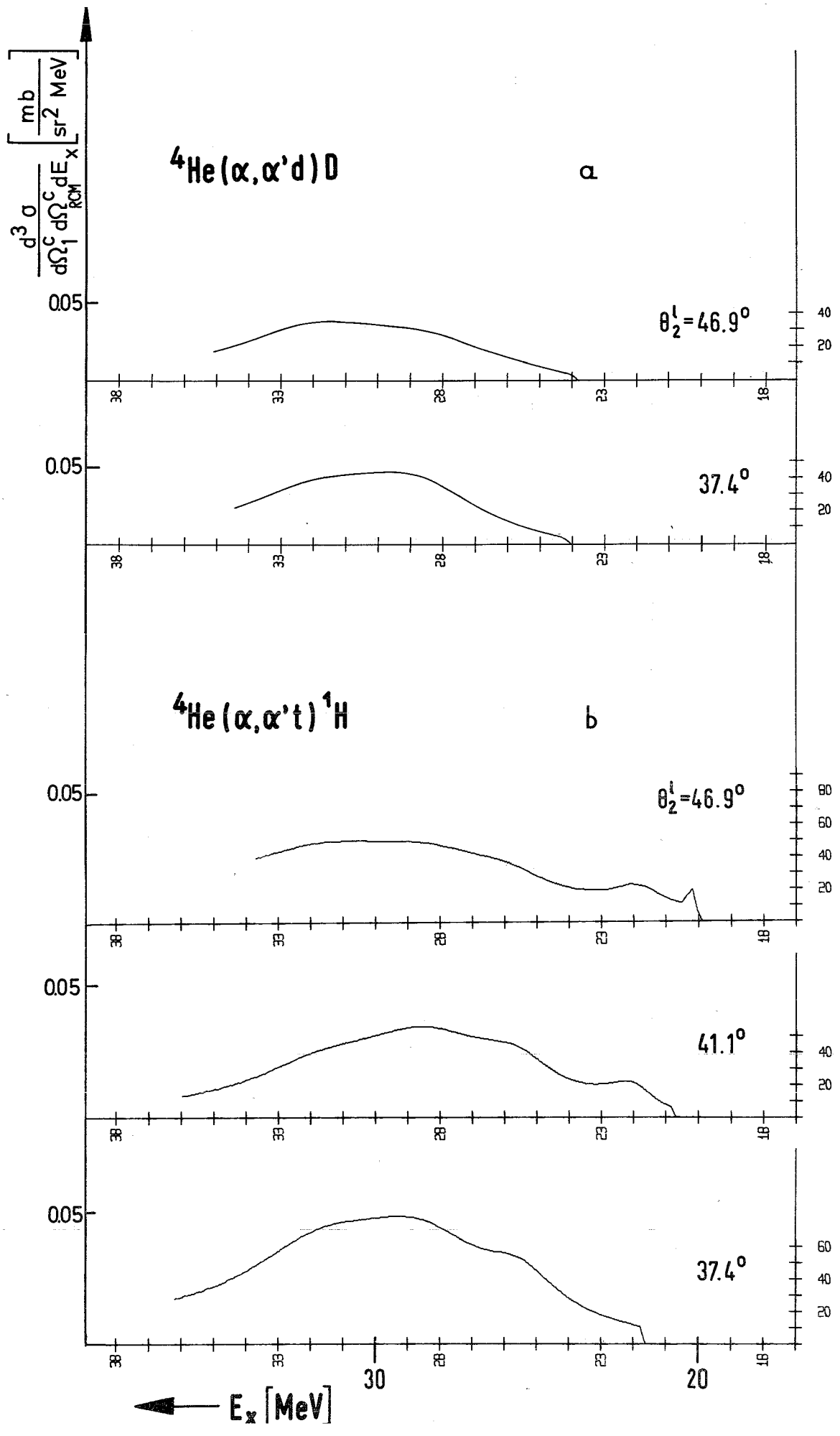

Fig. 7 Cross section in the RCM system as a function excitation energy, calculated with the parameters of the fits to the experimental data.

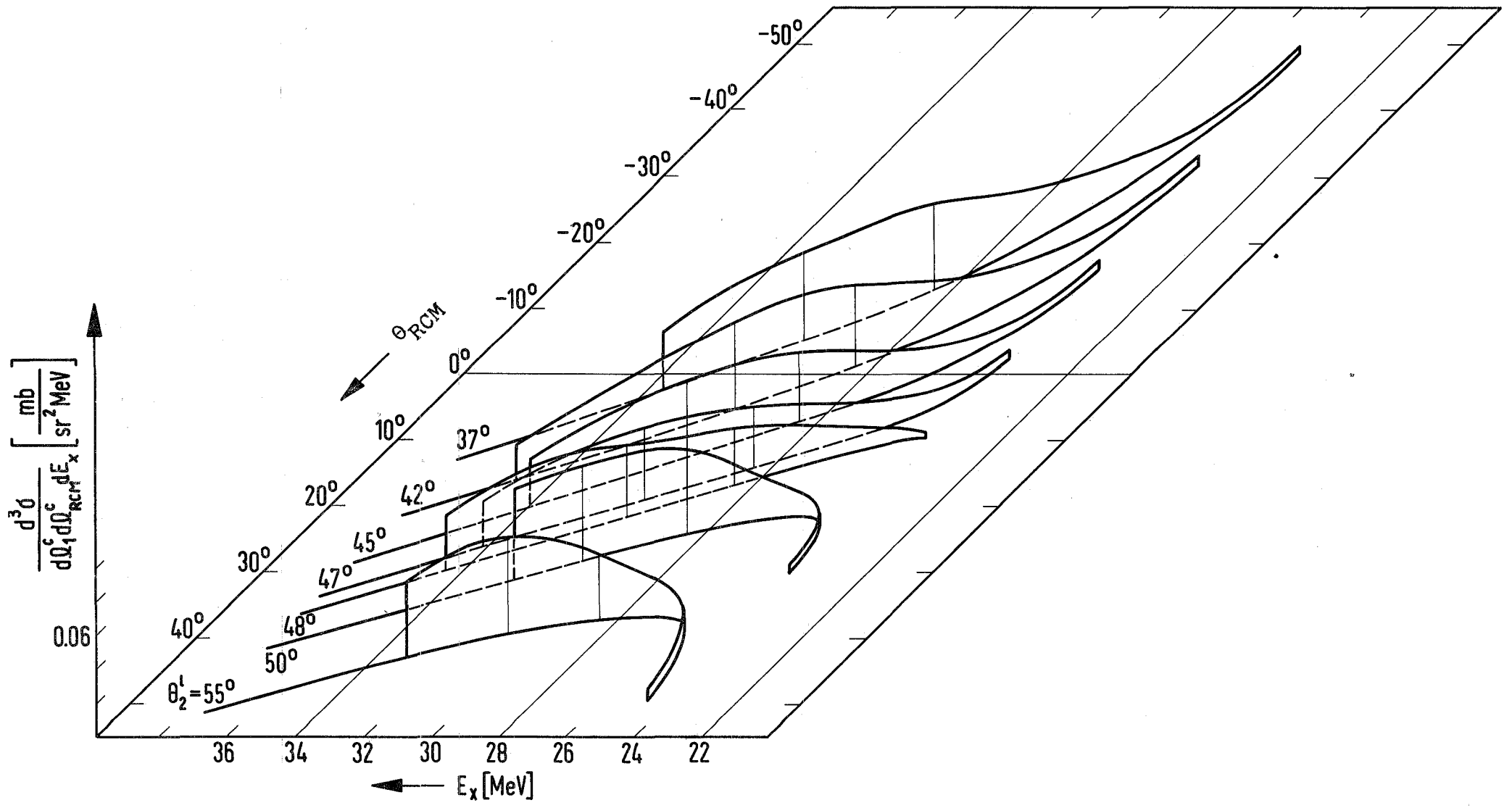

Fig. 8. Cross section in the RCM system, as function of the excitation energy and Θ_{RCM}, for the $^4He(\alpha,\alpha'd)D$ reaction.

The simplest assumption to account for the structure is to use two Breit-Wigner resonances. The resulting solid line in fig. 6 yields an excellent fit for two resonances at 28.7 MeV and 31.9 MeV. At the very least this assumption yields an excellent parametrisation of the data for transformation into the RCM system. To carry out the transformation the "theoretical" spectrum, not folded, is multiplied by the Jacobi factor for transformation from the laboratory to the RCM system. This can be obtained from eq.(10) in reference 10.

Note that the expresion of ref.10 has to be inverted! The corresponding spectra for $\theta_2^{\ell} = 37.4^{\circ}$ and $\theta_2^{\ell} = 46.9^{\circ}$ are shown in fig. 7a. Fig. 7b shows three representative RCM spectra for the $^4He(\alpha,\alpha't)^1H$ reaction.

Fig. 8 illustrates the result of a complete transformation into the RCM system. It is characteristic of the effect of the transformation for the reactions investigated in this paper. Here σ_{RCM} is plotted as a function of both E_x and Θ_{RCM}. With decreasing E_x the angular range of Θ_{RCM} widens, reflecting the decrease in the size of the decay cone. Also with increasing E_x the recoil axis ($\Theta_{RCM} = 0$) moves to smaller values of θ_2^{ℓ}. Note, for increasing Θ_{RCM}, that the distribution for the 28.7 MeV resonance drops gradually and that for the 31.9 MeV stays approximately isotropic.

To obtain acceptable fits to the upper and lower branch triton spectra, five resonances have to be assumed. In addition to the obvious ones at 20.2 and 21.9 MeV, a fairly weak one at 25.5 MeV is needed and two more at 28.3 and 31.7 MeV with parameters similar to those of the d,d channel. The values of the resonance parameters for simultaneous fits of the different families of spectra are listed and compared in table 1, section 3.7.

3.4 The $^4He(\alpha,\alpha'^3He)n$ Reaction

In fig. 9a representative set of spectra for the $^4He(\alpha,\alpha'^3He)n$ reaction is shown. From a consideration of charge symmetry of nuclear forces they are expected to be identical with the corresponding spectra of the T + p channel, except for the effects associated with the differing Q-values. This is indeed the case.

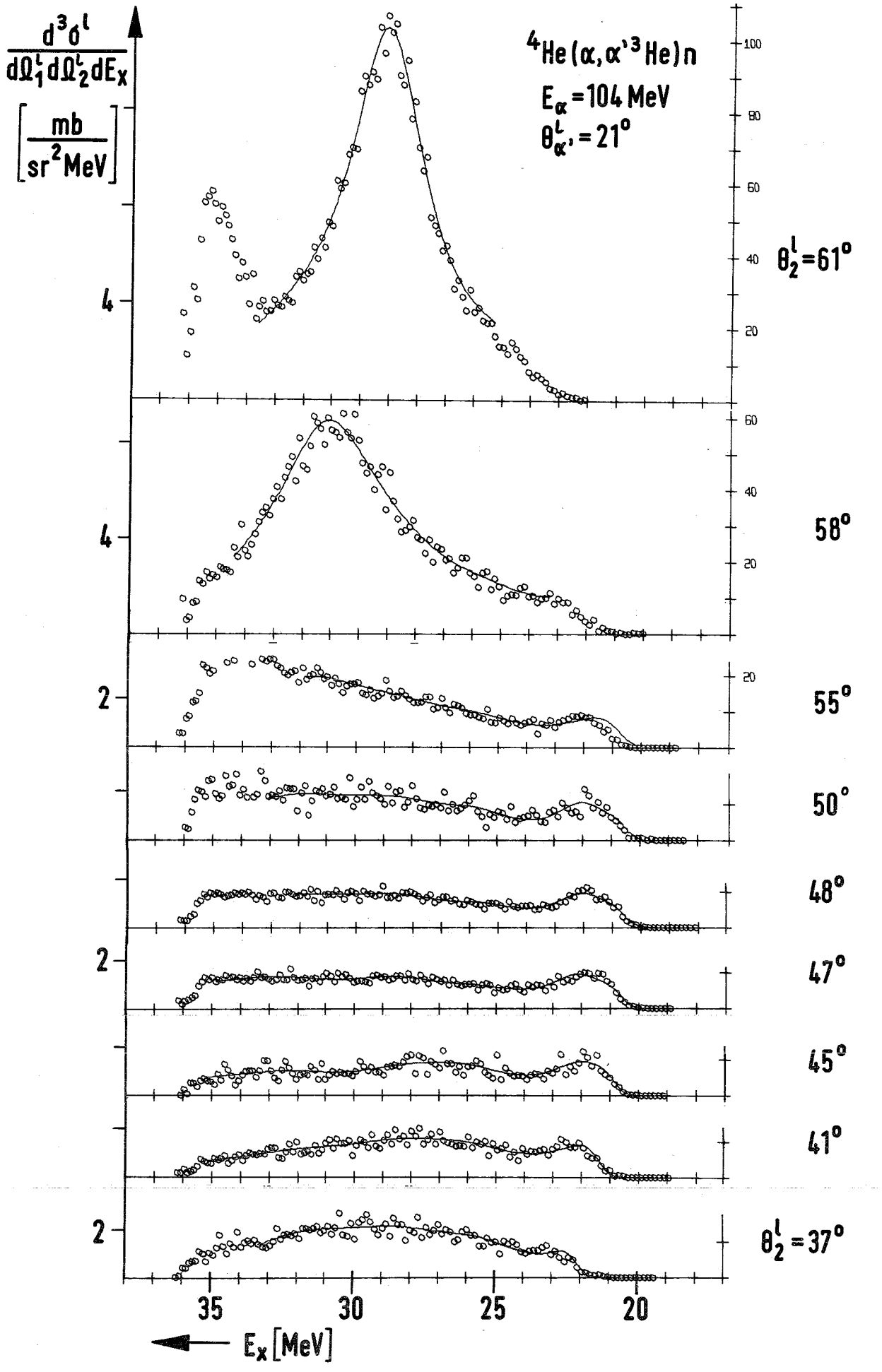

Fig. 9. Representative set of spectra for the $^4He(\alpha,\alpha'^3He)n$ reaction.

As it is below the threshold, the 20.2 MeV state cannot appear. This makes the 21.9 MeV resonance appear more distinct. A good fit can be obtained, as shown, using for the 21.9, 25.5, 28.3 and 31.7 MeV resonances the parameters determined for the T+p channel. The ^{5}He ground state appears at large angles more pronounced as it is narrower than the ^{5}Li ground state. The rise near E_x=35 MeV in the uppermost spectrum stems from the fact that this state also appears twice in the upper and the lower branch but with the role of the E_α, and $E_{^3He}$ axis interchanged.

3.5 The ^{4}He(d,d't)^{1}H and ^{4}He (d,d'd)D Reactions

Figure 10a gives a set of coincidence spectra for the upper branch of the ^{4}He(d,d't)^{1}H reaction. They are characterized by a single prominent distribution peaking at 21.2 MeV excitation and only weak structure above. The spectra for $\theta_2^\ell = 37^\circ$ corresponds to the recoil axis for 20.2 MeV excitation.

The 0^- state at 21.4 MeV [20]) is allowed in this reaction. An attempt to fit these spectra with a single Breit-Wigner resonance gave a very poor result. Two fits with different extreme assumptions were carried out; both gave equally acceptable fits:

a) Resonances at 21.9 and 21.1 MeV plus a weak one at 20.2 interfere with a significant non-resonant background,

b) the non-resonant background is assumed to be zero. Then one needs in addition to the ones above further resonances at 25.1, 28.6 and 31.4 MeV.

These latter fits are shown in fig. 10a. It is felt that this is more reasonable, as for all other reactions the nonresonant term was negligibly small and in this case the non-resonant term would certainly not be isotropic either. Incidentally the spectrum for $\theta_2^\ell = 25^\circ$ is beyond the edge of the decay cone for the 21.1 MeV resonance.

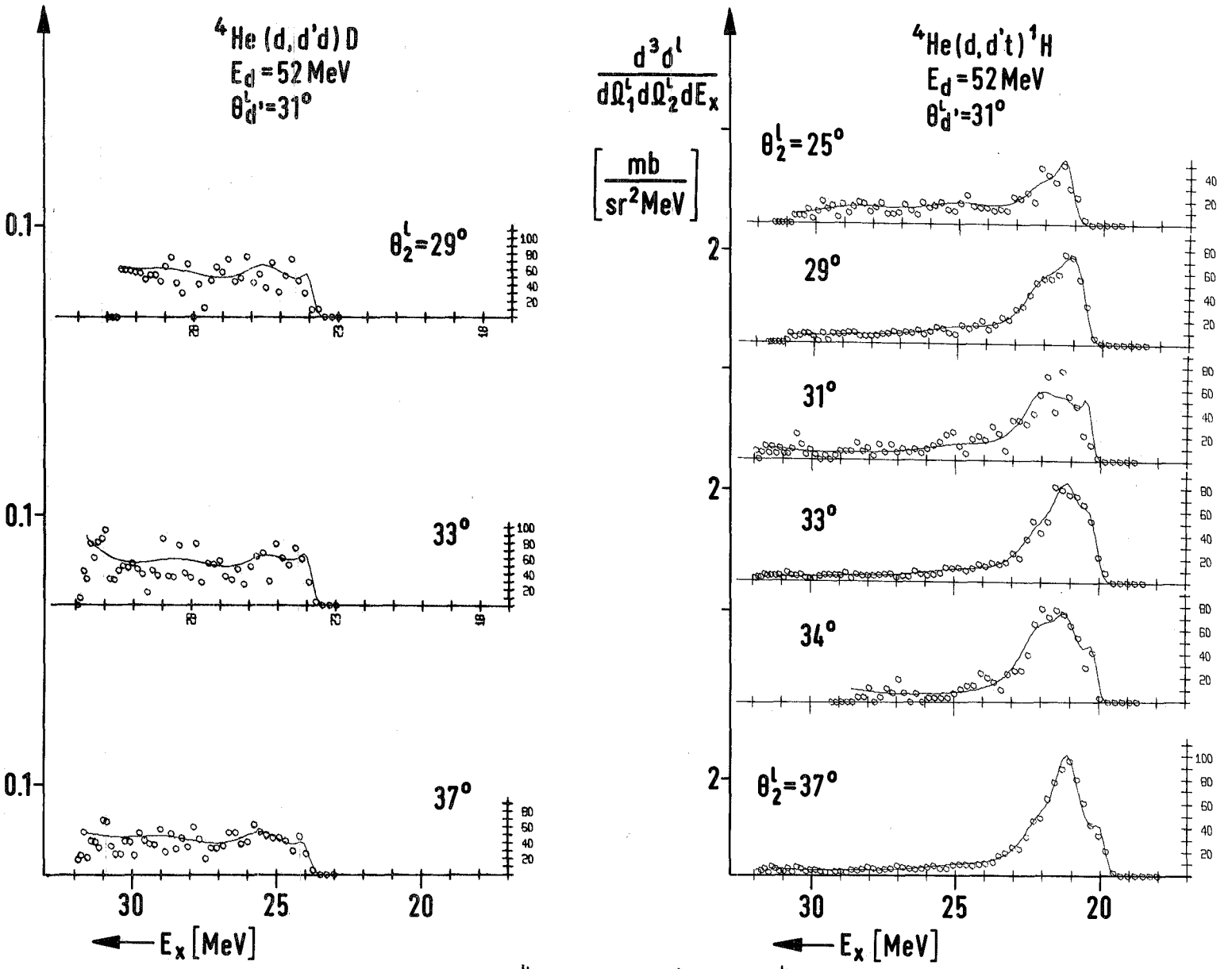

Fig. 10. Spectra for the ^{4}He(d,d't)^{1}H and ^{4}He(d,d'd)D reactions.

The only interfering reaction would be caused by T = 1/2 resonances of ^{3}He between 7.5 and 16 MeV excitation, shifting as noted before. However, no evidence was found for such resonances.

The neglect of interference between the 0^- and the 2^- level might be severe. In a singles spectrum there can be no interference between levels of different J^{π}, as the interference terms drop out upon integration over Ω_{RCM}.

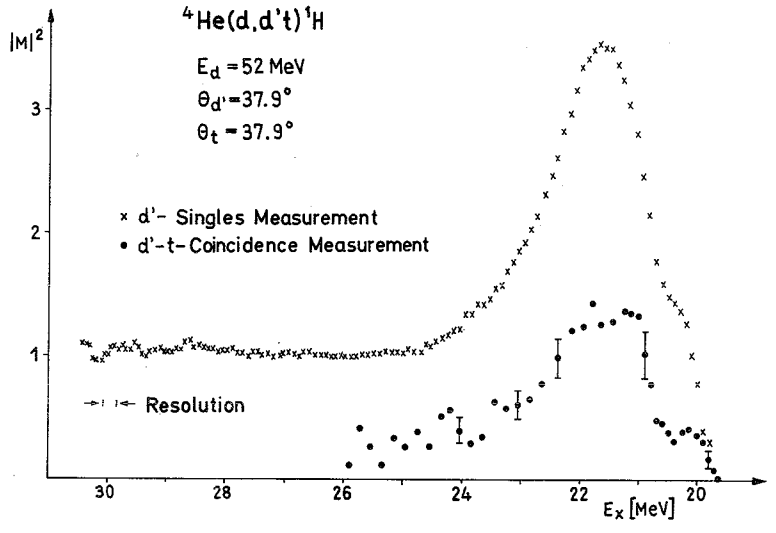

Fig. 11. Comparison of the ^{4}He(d,d') singles and the ^{4}He(d,d't)^{1}H coincidence spectra.

Fig. 11 shows for comparison a single and a coincidence spectrum for $\theta_1^{\hat{\ell}} = \theta_2^{\hat{\ell}} = 37.9^{\circ}$. Here in arbitrary units the square of the matrix element is shown, to eliminate the distortions due to different shape for the phase space distribution for singles and coincidence spectra. For this pair of angles the 20.2 MeV state is more pronounced, also the sharp drop near E_x = 21 MeV. The fit of several singles spectra confirms the parameters obtained from the coincidence spectra.

Three of the simultaneously measured spectra for the ^{4}He(d,d'd)D reaction are shown in fig. 10. They show little structure. These spectra can be adequatly fitted with the same resonances. The results are listed for comparison in table 1 in section 3.7.

3.6 Deuteron induced reactions on ^{6}Li

A third possibility to excite the T=0 states of ^{4}He is by bombarding ^{6}Li with deuterons. Recently results on the same reaction at lower energies have been published [14].

A comparison of the results shows the advantage of using higher incident energies, and at the same time demonstrates that even higher energies would be desirable in spite of the positive Q-value. All three decay channels are disturbed by other FSI (^{5}He, ^{5}Li, ^{6}Li), so that only limited portions of the angular correlations are clean, as far as ^{4}He resonances are concerned.

Fig. 12 shows a spectrum for the ^{6}Li(d,α't)^{1}H reaction. The fit yields no contribution from the 20.2 and 21.1 MeV states, a very prominant peak for the 21.9 MeV state and a weak indication for a 25.5 MeV state.

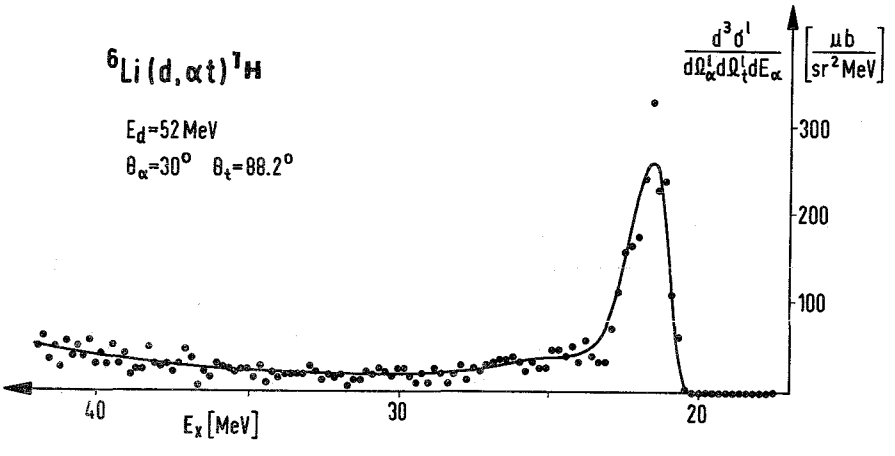

Fig. 12. Typical spectrum for the ^{6}Li(d,αt)^{1}H reaction.

Fig. 13 gives a set of four spectra for the ^{6}Li(d,d'd)D reaction. The bottom two spectra show the 25.5 MeV resonance quite strongly, plus a weaker distribution around 28.5 MeV. The peak at high excitation energies arises from the 4.57 MeV state of ^{6}Li. As θ_2^{ℓ} decreases the quasielastic peak starts to obscure the FSI peaks.

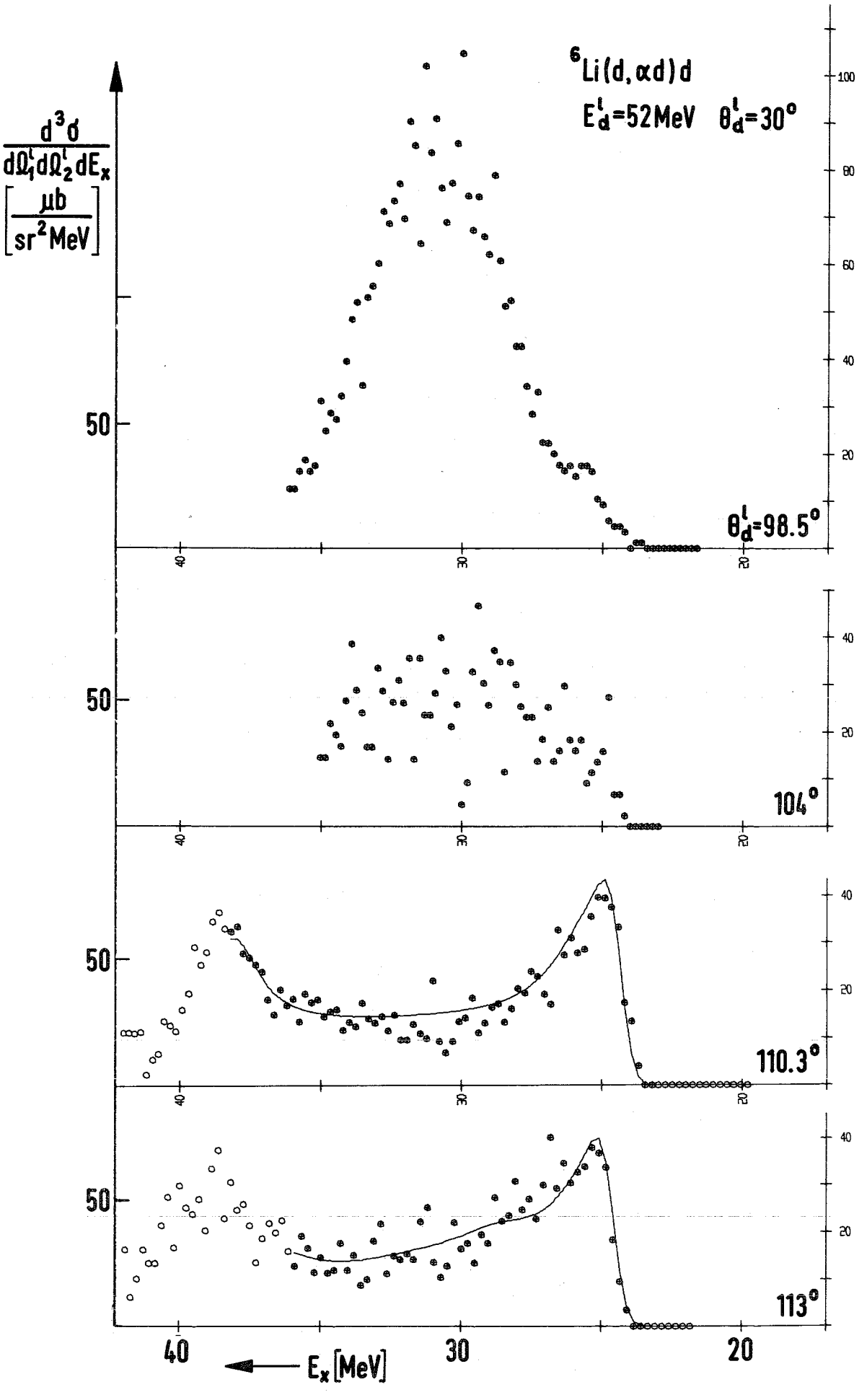

Fig. 13. Spectra for the ^{6}Li(d,αd)D reaction showing the 25.5 MeV state. For smaller values of θ_d^l, the quasielastic process dominates.

A narrow 2^+ level 55 keV above the (d,d) threshold has been reported by Franz and Fick [23]). The present reaction should be very suitable to populate such a state, being interpreted as consisting of two deuteron clusters. The proximity to the threshold would cause a significant fraction of the particles decaying into 4π to enter $\Delta\Omega_2^\ell$ of the second detector. This resonance should show up as a narrow line with the experimental resolution of 2.5 channels just above the threshold for the spectrum at $\theta_2^\ell = 98.5^\circ$. The angle $\theta_2^\ell = 104^\circ$ is outside the decay cone. The comparison of these spectra permits us to give an upper limit of 25 nb/sr^2 for the cross section for excitation of such a narrow resonance in this reaction. A corresponding value for the 25.5 MeV resonance is about 4 μb/sr^2.

3.7 Summary of the results on resonance parameters

The data presented in the previous subsections show that for a given reaction only the measurement of an angular correlation θ_2^ℓ permits one to detect or to exclude, interference from other FSI or the quasielastic scattering. For a fixed θ_1^ℓ the ^{4}He resonances are stationary, whereas in general interfering processes shift with changing θ_2^ℓ, and can thus be identified with the help of kinematics.

We have measured eight such correlations for three entrance and three decay channels. For a given correlation those spectra or parts of spectra that are free from interfering reactions were treated as follows:

1) Simultaneous fits minimizing χ^2 were carried out using formula (3). In these fits the positions E_n as well as widths Γ_n for each resonance were varied in common, and the A_n, B_n and C_n were varied individually for each spectrum. In fitting, the minimum number of resonances were used that reproduced the data and gave an acceptable fit.

2) The resulting parameters are listed in table 1.
A subjective estimate for the error in position is ± 10% of the width, in addition to ± 60 keV for the uncertainly in the primary energy and θ_1^ℓ, and for the relative error in the widths ± 15%.

T = 0	^{4}He(α,α' t)^{1}H	^{4}He(α,α' ^{3}He)n	^{4}He(α,α' d)D	^{4}He(d,d' t)^{1}H	^{4}He(d,d' d)D	^{6}Li(d,α' t)^{1}H	^{6}Li(d,α' ^{3}He)n	^{6}Li(d,α' d)D
20.2 0^+	20.2±0.004 Γ=0.2±0.006	-	-	20.2±0.03 0.2±0.01	-	not observed		-
21.1 0^-	forbidden		-	21.1±0.02 0.8±0.04	-	not observed		-
21.9 2^-	21.9±0.017 Γ=1.8±0.01	21.9±0.02 1.9±0.05	-	22.0±0.03 1.8±0.06	-	21.9±0.04 1.8±0.08	consistent with other values	-
25.5 $(0^+,1^+)$	25.5±0.02 Γ=2.9±0.01	25.6±0.06 3.1±0.12	at most weak	25.1±0.04 2.9±0.2	25.2±0.02 2.2±0.01	weak, consistent		25.5±0.12 3.0±0.22
28.5 1^-	28.3±0.02 Γ=5.3±0.01	28.3±0.03 5.3±0.07	28.7±0.01 5.0±0.13	28.6±0.04 3.8±0.34	28.7±0.03 4.6±0.02	weak, consistent		weak, consistent
31.8	31.7±0.02 Γ=5.6±0.01	31.7±0.05 5.5±0.01	31.9±0.07 5.9±0.02	31.4±0.19 2.8±0.53	31.9±0.04 4.9±0.03	very weak, consistent		very weak
Number of spectra fitted	14+8	13	14	6	3	8	3	2

Comparison of resonance positions and widths obtained in fitting data from 8 reactions. A dash means that the level is below threshold. Errors derived from error matrix, to indicate sensitivity of statistics only.

Table 1

The errors given in table 1 are the values derived from the diagonal elements of the error matrix. As can be seen the values for E_n, Γ_n agree for all 8 reactions within the errors. Thus the resonance parameters are internally consistent.

They are also in reasonable agreement with those resulting from the phase-shift analyses [8]), given in fig. 14. The 28.5 MeV, 2^+ level shown dashed there is associated with a rise in the d-wave phase, but the interpretation is not unique [22]). For comparison

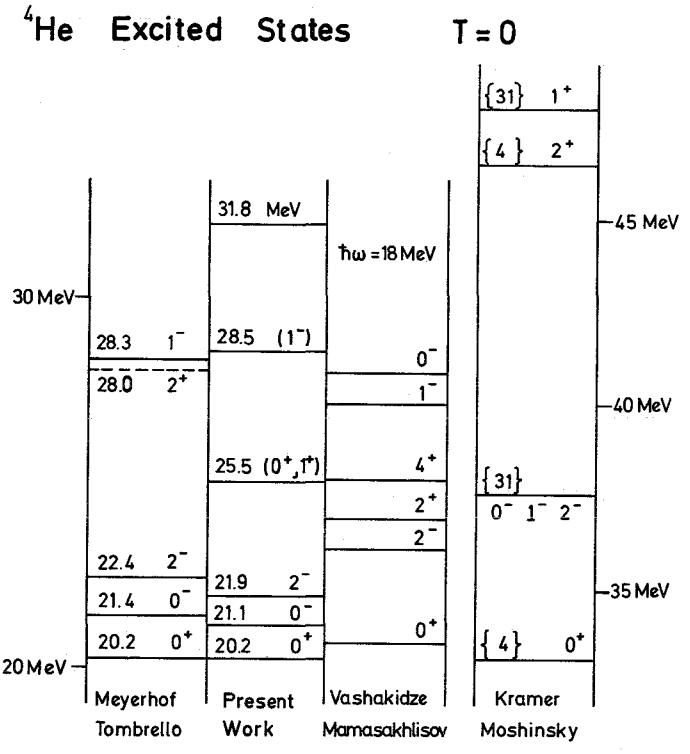

Fig. 14. Energy level diagram for T=0 states in ^{4}He.

two theoretical predictions are also shown. In the work of Kramer and Moshinsky [2]) only central forces were used and hence the $\ell = 1$, $S = 1$ triplet is degenerate. In the paper by Vashakidze and Mamasakklisov [4]) this triplet is split up by spin-orbit forces and gives the Landé 2^-, 1^-, 0^- sequence. To obtain the experimentally observed 0^-, 2^-, 1^- ordering, strong tensor forces are needed [3]).

The 25.5 MeV level is new. While it is rather weakly excited in the inelastic scattering off ^{4}He, it shows up clearly in the ^{6}Li(d,α'd)D reaction. There is indication for such a level in the ^{4}He(α,α') singles spectra [24]). The 31.8 MeV level is required in fitting most of the spectra, though it does not strongly protrude in any of them. In any case its inclusion permits an excellent parametrisation of the data.

Except possibly for the ^{4}He(d,d't)^{1}H reaction we observed that the non-resonant term (coefficient C in eq. (3) was either zero, or contributed only a few percent to the cross section. Forcing C = 0, and hence all interference terms A_n = 0, increased χ^2 by only 10 to 15%, while the number of parameters is reduced by a factor of about two. This further restriction A_n = C = 0, which one would not generally expect to hold, has been used in the following discussion.

4. The angular correlations

Having consistently interpreted our data from eight reactions in terms of a set of six resonances, let us consider the decay angular correlations. We have measured angular correlations of the decay particles from five excited states of ^{4}He.

To simplify as noted we forced the C and hence the A_n coefficients to be zero in the fits. For each family of spectra the resulting fit provided a set of coefficients $B_n(\theta_2^\ell)$ for each resonance n and angle θ_2^ℓ. The area underneath each resonance is given by $2\pi\ B_n$. These coefficients, when multiplied by the appropriate Jakobi factor at the centre of the resonance yield the angular correlations in the RCM system as shown in fig. 15 and 16. The error bars shown are calculated from the diagonal terms of the error-matrix. They give that variation of a given parameter, which increases the χ^2 value by unity, when all other parameters are held constant.

Figure 15a) shows the correlation for the ^{4}He(α,α't)^{1}H reaction for the 20.2 MeV, 0^+ state. If the reaction mechanism is sequential, the distribution for a J = 0 state must be isotropic, as borne out.

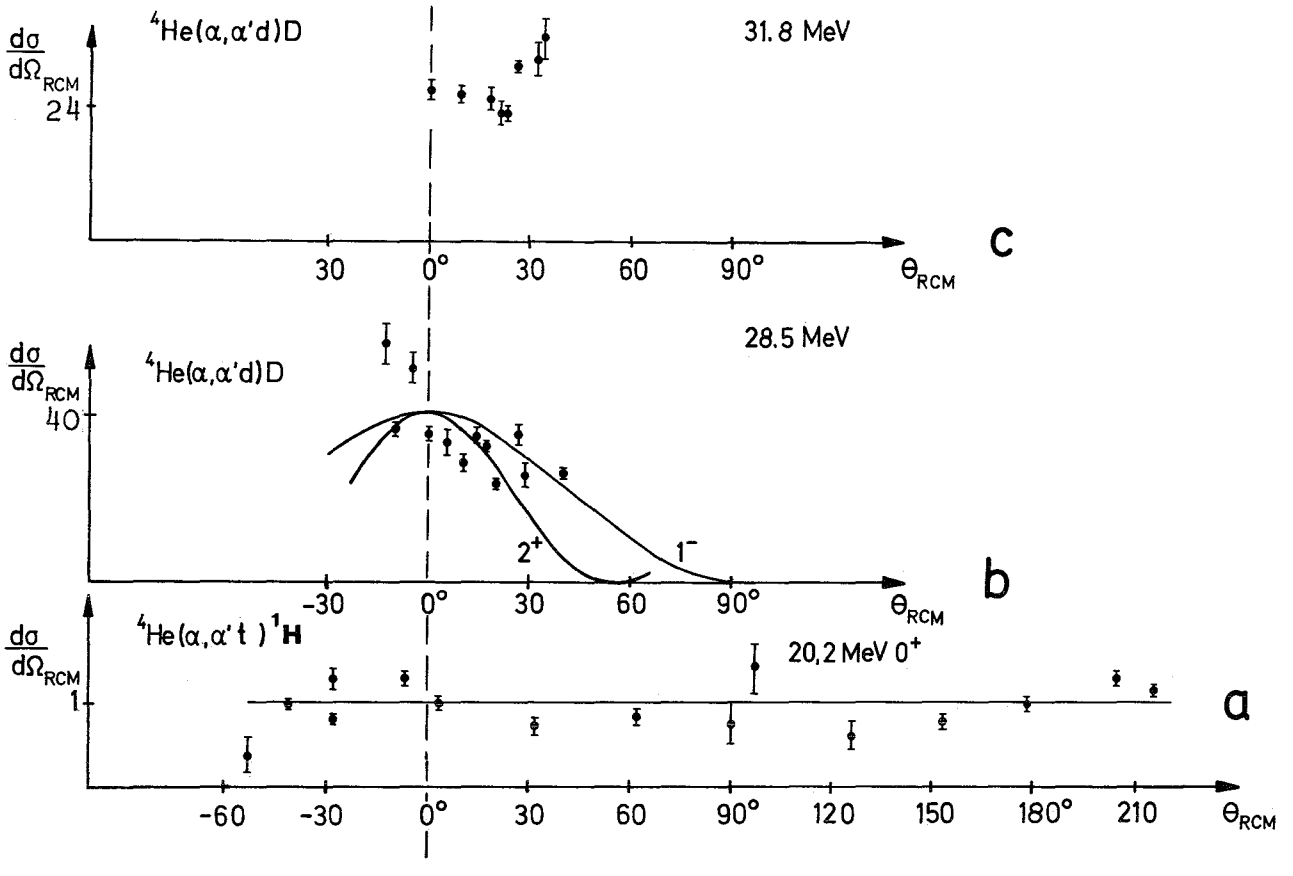

Fig. 15. Angular Correlations in the RCM system for $\theta_1^{\ell}=21^{\circ}$. One unit corresponds to about 100 μb/sr^2.

The points around 0° stem from the upper branch, and those around 180° from the lower branch. As the decay cone for this state is rather small, the points near ± 90° carry a correction for the azimuthal angular opening, and the error bars have been doubled.

Fig. 16 shows the angular correlations for the 21.9 and the 25.5 MeV resonances, both for the $^4He(\alpha,\alpha't)^1H$ and the $^4He(\alpha,\alpha'^3He)n$ reactions. As expected from charge symmetry both should yield identical results. The 25.5 MeV resonance is isotropic so far as one can tell. As the channel spin in the exit channel can only

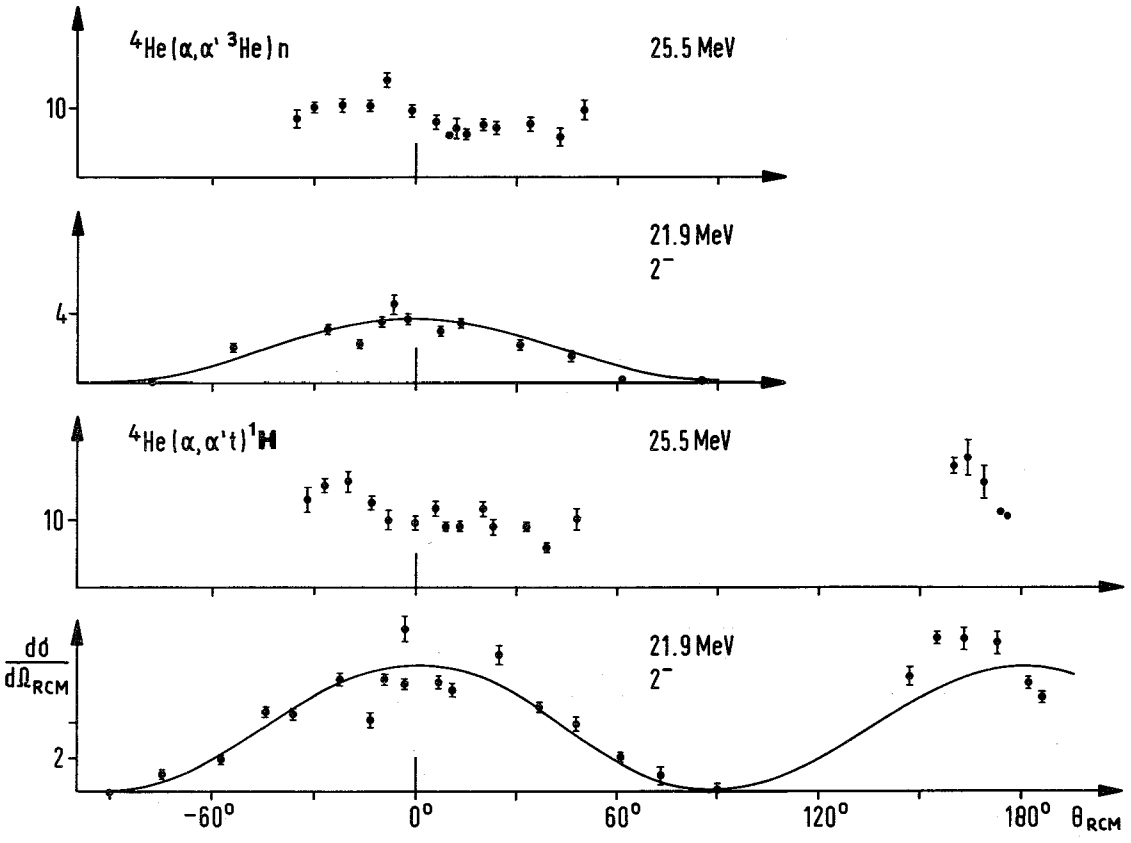

Fig. 16. Angular correlation in the RCM system for $\theta_1^{\ell} = 21^{\circ}$. One unit corresponds to about 100 μb/sr^2.

be 0 or 1, the isotropy implies $J^{\pi} = 0^+$ or 1^+ (as 0^- is forbidden) within the validity of our assumptions. A third 0^+ state near 25 MeV has recently been predicted by Hutzelmeyer [16].

The 21.9 MeV, 2^- level has non-normal parity, with channel spin S = 1. Its excitation is forbidden in the ordinary theories [17] of inelastic α-particle scattering. The PWBA only permits excitation of natural parity states; within the L-S coupling-scheme normal parity S = 1 states are also forbidden.

We have calculated the angular correlations using the impulse approximation with the following simplifying assumptions. The projectile interacts with only one cluster component of the target, say a neutron, whereas the ^{3}He-components acts as spectator. The scattering amplitude t is taken to have the same form as in n - α scattering on the energy shell

$$t = a + b\ \vec{\sigma}_1 \cdot \vec{n} \qquad (5)$$

where $\vec{\sigma}$ is the neutron spin and $\vec{n}$ the normal to the scattering plane and we assume the variations in the functions a and b to be negligible when the spectator momentum varies over the regions of momentum space which make significant contributions to the reaction. With these assumptions and with b vanishing allows the excitation of the same levels and predicts the same angular correlations as the zero range PWBA. With b non-zero S = 0 to S = 1 transitions are induced. It populates coherently the $m_J = \pm 1$ substates when the quantisation axis is chosen along the recoil axis. The decay into ^{3}He - n or T + p is via L = 1, channel spin 1. For both the $J = 1^-$ and $J = 2^-$ states the angular correlation is given by $d\sigma/d\Omega_{RCM} = \text{const } (\cos^2\theta_{RCM} + \sin^2\theta_{RCM} \sin^2\phi_{RCM})$ where ϕ_{RCM} is measured relative to the reaction plane.

In the reaction plane the experimental points agree well with the $\cos^2\theta_{RCM}$ distribution shown in fig. 16. Perpendicular to the reaction plane the distribution should be isotropic. A further result of the theory is that interference between 1^- and 2^-, S = 1 states only effects the amplitude but not the shape of the distribution in the reaction plane.

Also note that the distributions are symmetric about the recoil axis ($\theta_{RCM} = 0^o$) as predicted by the zero range PWBA, as well as the present theory.

Fig. 15b shows as far as available the distribution for the 28.5 MeV level for the ^{4}He(α,α'd)D reaction. Drawn in are the $\cos^2\theta$ distribution for a S = 1, $J^\pi = 1^-$ state and the PWBA prediction for L = 2, S = 0, $J^\pi = 2^+$ [25]). The data points favor the 1^- distribution.

Fig. 15c gives the points for the 31.8 MeV resonance. They are consistent with an isotropic distribution. The 28.5 and 31.8 MeV distributions for the ^{3}He + n and T + p channels have the same shape, but for the largest values of θ_{RCM} they are masked by the mass 5 resonances.

For the 20.2, 21.9 and 28.5 MeV resonances our results on J^π are consistent with those of Meyerhof and Tombrello [8]). The 25.5 MeV level has not been previously observed. Whether the resonance at 31.8 MeV, which we need to fit our data, is associated with the rise in the d-wave coefficients up to 30 MeV observed in the phase-shift analysis, is not clear. It has been shown [22]) that this does

not necessarily imply a 2^+ state. There remains the question of the validity of our neglect of interference between resonances. This can be answered only by iteration, as one has to know J^π and channel spins. If our interpretation of the 21.9 and the 28.5 MeV levels is correct, they do not interfere with each other; also they have S = 1. The 20.2, 25.5 and 31.8 MeV resonances all appear to be isotropic. If, as the 20.2 MeV resonance is known to be, all are S = 0, then interference occurs only between non-adjacent resonances, as different channel spins do not interfere.

5. Discussion and conclusions

Resonances arising in FSI lend themselves to a fairly simple interpretation if the reaction mechanism is that of sequential decay.

Validity of the sequential reaction mechanism is taken to mean that the decay of the intermediate system is independent of its formation. The decay should then proceed according to the same laws that govern the decay of a compound nucleus. In particular the level parameters are a property of the compound system and do not depend on formation or decay. The branching ratios in the decay do not depend on the method of formation. For sequential decay through an isolated level there must also be invariance of the Θ_{RCM} dependence of the angular correlation under a rotation by 180^o on account of parity conservation [26]).

To test the validity of the sequential decay mechanism we have measured angular correlations for three different entrance channels and the three possible exit channels. The following findings support the mechanism of sequential decay:

1) All entrance and exit channels investigated give resonant positions and widths that are consistent within the experimental errors. The resonance parameters are a property of the intermediate system only; no dependence on Θ_1^ℓ or Θ_2^ℓ was observed.

2) Within the experimental errors the three angular correlations checked were found to be invariant under a rotation by 180^o about the normal to the reaction plane. $\Theta_{RCM} \rightarrow \Theta_{RCM} + 180^o$

3) A further test constitutes the evaluation of the branching ratios for the decay of the intermediate system into the different channels. This has not yet been done; however, the branching ratios do not appear to be crudely out of line.

As regards both positions and widths and information on spin and parity our results are consistent with what has been previously known about T=0 states of ^{4}He [8].

The present data facilitate more precise determinations of positions and particularly widths of the resonances.
We found evidence for an additional state at 25.5 MeV. The isotropy of its angular correlation suggests $J^{\pi} = 0^{+}$ or 1^{+}. If, as has been predicted by Hutzelmeyer [16], this is a 0^{+} state with a strong component of L = 2, S = 2, one can understand the fact that it has not been seen in the phase-shift analysis of low energy scattering and reactions.

It is interesting to compare the phase-shift analysis method with the one used in the present investigation.

The experimental difficulties of carrying out a coincidence measurement are compensated by the yield of spectra covering a large range of excitation energies starting at the threshold. The added recoil energy makes the simultaneous measurement of the various decay channels readily possible. The present method offers higher selectivity in many cases. It is applicable even when for lack of a stable target the phase-shift analysis cannot be carried out. However, particularly at low incident energies, one does have to concern oneself with possible interference from other FSI and the quasielastic scattering.

The energy spectra show more structure, and so are easier to interpret. See reference [18] for instance. This is attributed to the fact that in the formation of the intermediate system Coulomb and centrifugal forces and more importang the non-resonant terms play less of a role. The level widths obtained in the present work are significantly smaller than those used by Meyerhof and Tombrello. This effect has been previously noted [19].

The angular correlations in the RCM system are determined by the population of the magnetic substates of the levels. Except for simple cases such as isotropy, they depend on the reaction mechanism. The symmetry of the angular correlations about the recoil axis ($\Theta_{RCM} = 0$) is predicted by the zero range PWBA as well as the theory described in section 3.2. It is gratifying to observe that these simple models account for the experimental data. In general this symmetry is not required for a sequential reaction mechanism. It remains to be shown under what conditions such models constitute and adequate description, and permit the use of the method to determine spins and parities. Measurements on heavier nuclei are in progress to test this point.

The authors want to express their gratitude to Prof. A. Citron, Prof. W. Heinz and Prof. H. Schopper for their encouragement and support.

The good cooperation with Dr. G. Schatz and the members of the cyclotron staff is gratefully acknowledged.
We would like to thank Mr. W. Siebert for help with the experiment and the programming.

References

1) A. de Shalit and T.D. Walecka, Phys.Rev. 147 (1966) 763

2) P. Kramer and M. Moshinsky, Phys.Lett. 23 (1966) 574

3) B.R. Barrett, Phys.Rev. 154 (1967) 955

4) I.Sh. Vashakidze and V.I. Mamasakhlisov, Sov.Journ.Nucl. Phys. 6 (1968) 532

5) T.T.S. Kuo and J.B. McGrory Nucl.Phys. A134 (1969) 633

6) P.P. Szydlik, Phys.Rev. C1 (1970) 146

7) E.O. Alt, P. Grassberger and W. Sandhas, Phys.Rev. C1 (1970) 85

8) W.E. Meyerhof and T.A. Tombrello, Nucl.Phys. A109 (1968) 1

9) E.L. Haase et al., Proc. Int. Conf. Clustering Phenomena in Nuclei, Bochum IAEA Vienna (1969) p. 223

10) G.G. Ohlsen, Nucl.Instr.Meth. 37 (1965) 240

11) M.L. Goldberger and K.M. Watson, Collision Theory (Wiley, New York, 1964) p. 540 ff

12) C.A. Levinson and M.K. Banerjee, Ann.Phys. 2 (1957) 471

13) J. Humblet and L. Rosenfeld, Nucl.Phys. 26 (1961) 529

14) J.C. Legg et al. Nucl.Phys. A119 (1968) 209

15) P.A. Assimakopoulos et al., Nucl.Phys. A144 (1970) 272

16) H. Hutzelmeyer, private communication

17) W.W. Eidson and J.G. Cramer Jr., Phys.Rev.Lett. 9 (1962) 497

18) M.D. Goldberg, Prog. in Fast Neutron Physics, G.C. Phillips, J.B. Marisu and J.R. Risser eds., The University of Chicago Press, Chicago (1963) p. 3

19) V.V. Komarov and H.A. Salman, Phys.Lett. 31B (1970) 52

20) C. Werntz and W.E. Meyerhof, Nucl.Phys. A121 (1968) 38

21) ibid, p. 60

22) W.E. Meyerhof et al., Nucl.Phys. A148 (1970) 211
W.E. Meyerhof et al., Nucl.Phys. A131 (1969) 489

23) H.W. Franz and D. Fick, Nucl.Phys. A122 (1968) 591

24) E.E. Gross et al., Phys.Rev. 178 (1969) 1584

25) H.B. Willard et al. in Fast Neutron Physics, J.B. Marion and J.L. Fowler eds., Interscience Publishers, New York (1963) p. 1217 ff

26) C. Zupančić, Few Nucleon Problems (Fed.Nucl.Energy Commission of Yugoslavia, Hercegnovi, 1964) Vol. II, p. 61